Cell Proliferation

Cell Prolif., 2014, **47**, 133–145 doi: 10.1111/cpr.12094

IKVAV regulates ERK1/2 and Akt signalling pathways in BMMSC population growth and proliferation

B. Li, T. Qiu, P. Zhang, X. Wang, Y. Yin and S. Li

State Key Laboratory of Advanced Technology for Materials Synthesis and Processing, and Biomaterials Science and Engineering Research Center, Wuhan University of Technology, Wuhan, 430070, China

Received 10 September 2013; revision accepted 8 November 2013

Abstract

Objectives: The molecular mechanism of bone marrow mesenchymal stem cell (BMMSC) population growth and proliferation, induced by Isoleucyl-lysyl-valyl-alanyl-valine (IKVAV), was explored in this study.

Materials and methods: IKVAV peptides were synthesized by the solid-phase method. Influence of IKVAV on BMMSC population growth and proliferation were investigated by assays of CCK-8, flow cytometry, real-time PCR and western blotting.

Results: IKVAV peptide was found to induce proliferation and proliferating cell nuclear antigen (PCNA) synthesis of BMMSC in a dose- and time-dependent manner. Cell cycle analysis showed that the proportion of IKVAV-treated BMMSC in S phase in was higher than controls. Western blot results suggested that mitogen-activated protein kinase/extracellular signal-regulated kinase (MAPK/ERK) and phosphatidylinositol 3-kinase/protein kinase B (PI3K/Akt) signalling pathways were activated by IKVAV by enhancing phosphorylation levels of ERK1/2 and Akt in the BMMSCs. Meanwhile, phosphorylation levels of ERK1/2 and Akt were partially blocked by ERK1/2 inhibitor (PD98059) and Akt inhibitor (wortmannin), respectively.

Conclusions: Our results demonstrated that IKVAV stimulated BMMSC population growth and proliferation by activating MAPK/ERK1/2 and PI3K/Akt signalling pathways. This study is the first to reveal an enhancement effect of IKVAV peptide on BMMSC at the signal transduction level, and the outcome could provide experimental evidence for application of IKVAV-grafted scaffolds in the field of BMMSC-based tissue engineering.

Correspondence: Y. Yin, State Key Laboratory of Advanced Technology for Materials Synthesis and Processing, and Biomaterials Science and Engineering Research Center, Wuhan University of Technology, Wuhan 430070, China. Tel.: + 86 27 87651853; Fax: + 86 27 87880734; E-mail: yinyixia@whut.edu.cn

Introduction

Mesenchymal stem cell (MSC)-based therapy is a promising strategy in the fields of regenerative medicine and tissue engineering (1,2). Promoting MSC proliferation has wide applications in stem cell therapies, particularly in the area of regenerative medicine, for such as diabetes mellitus (3), cardiac (4,5), liver (6–8), kidney (9,10), bone (11,12) and autoimmune diseases (13,14). So far, no critically adverse effects due to MSC-based implantation have been reported in clinical studies, which implies that their application in therapeutics is considered to be safe (15–18).

To promote MSC adhesion and growth, artificially simulated extracellular matrix (ECM) needs to be designed carefully to provide a cell-favourable environment. The ECM provides not only a physical substrate that can be grafted with specific ligands for cell adhesion and migration, but also with a variety of growth factors to stimulate cell proliferation and function. It is reasonable to expect that a synthetic ECM scaffold plays a similar role to promote tissue regeneration *in vitro* as does native ECM *in vivo*. Due to cell viability and behaviour being drastically affected by chemical and mechanical properties of the surrounding environment, application of synthetic ECM for tissue engineering and cell-based therapies has gained significant momentum. Synthetic scaffolds for cell adhesion and delivery have been developed to improve cell function and anchoring at lesions (19). However, there are problems in application of cell-based regenerative therapy, such as poor cell viability, failure in their relocation to targets and low efficiency of engraftment (20,21). Moreover, most scaffold materials used in tissue engineering have failed to

provide active sites for cell anchoring due to their limitation in bioactivity. This may lead to inferior cell adhesion, as MSCs are sensitive to anchorage-dependent survival and regulation of apoptosis (22–24).

Thus, development of a bioactive scaffold to provide a microenvironment to support function and promote cell adhesion, growth and proliferation is one of the most emergent challenges of recent decades (25). Short peptide sequences (complex organic micromolecules containing carbon, hydrogen, nitrogen, oxygen and sulphur), have displayed clear advantages in large-scale chemical production and degradation, which reduce risk of immunogenicity and transmission of pathogens from necessary biological sources of full-length proteins (19,26). A number of laminin-derived short bioactive sequences, such as Isoleucyl-lysyl-valyl-alanyl-valine (IKVAV), YIGSR, and RNIAEIIKDI, function to encourage cell attachment and growth (27–29) and synthetic biomaterials are being designed to integrate bioactive ligands within hydrogel scaffolds for promoting cell response, and assimilation within the matrix. With increasing understanding of roles of growth factors, cytokines and their interactions with components of the ECM, novel biomaterials whose composition closely mimic natural tissue environments are being developed. This results in increased efficacy in the field of tissue repair and regeneration. Inherent biocompatibility and cell signalling capabilities of peptides have led to development of a broad range of functional materials with potential for many novel therapies. However, traditional 2-D artificial scaffolds or tissue culture dishes are not able to create a suitable platform for cell–cell interactions as does the ECM *in vivo*. Previous research has indicated that cell culture in 3-D scaffolds provides larger surface areas for cell attachment and proliferation, than do 2-D scaffolds (30–32). Peptide-based 3-D hydrogel scaffolds can more precisely mimic porosity and nanostructure of native ECM and can more readily incorporate signalling epitopes for cell–cell and cell–tissue interactions. Using bioconjugation techniques and orthogonal chemistry, peptide-based 3-D hydrogel scaffolds with multiple signalling molecules, such as cell-adhesion ligands, protease sensitive domains, growth factors and cytokines, can be readily modified to adjust a wide variety of biologically relevant signals, for enhanced therapeutic function and tissue regeneration (19). In novel 3-D hybrid scaffolds, which incorporate collagen sponge self-assembled peptide amphiphile nanofibres with MSCs, cell behaviour more closely resembles the *in vivo* environment and cells have significantly enhanced proliferation and differentiation characteristics than *in vitro*. Also, *in vivo* osteogenic differentiation compared to conventional static tissue culture plating is better in 3D (33,34). Thus, as an effective strategy for tissue repair, 3-D hydrogel scaffolds have been widely used in regeneration of bone, enamel, cartilage, central nervous system, transplantation of islets, wound-healing, and vascularisation and cardiovascular therapies (32,35–37).

As new kinds of biomaterials, evaluation of biocompatibility (determined by cell and tissue responses to IKVAV peptide-modified scaffolds *in vivo* and *in vitro*), was carried out. IKVAV peptide sequences were covalently attached to an aminated polymer surface using carbodiimide chemistry. This study indicates that IKVAV-treated surfaces displayed significantly higher numbers of adipose-derived stem cells (ASCs) bound in more spread out morphology, after 2 and 3 days cell seeding. IKVAV has potential applications to further promote attachment of ASCs to biocompatible scaffolds (38). Mi-GQASSIKVAV was coupled to a thiolated form of methacrylamide chitosan. Covalent modification of methacrylamide chitosan scaffold made it porous and biodegradable, and significantly improved neuronal adhesion and neurite outgrowth (39). RGD peptide conjugated to IKVAV peptide fibrils can be used as a basement membrane mimetic for promoting fibroblast adhesion, and used as a bio-adhesive scaffold for tissue engineering (40) and chemical modification of 3-D collagen scaffolds with both RGD and IKVAV peptides has been shown to significantly enhance cell adhesion over all other 3-D collagen matrixes (41). In *in vivo* evaluation, Matsuda *et al.* (42) have developed a new artificial guiding tube scaffold for nerve regeneration consisting of molecularly aligned chitosan with IKVAV and YIGSR bonded covalently. Their results indicated that structure of tendon chitosan and biological activity of intact laminin peptides were well maintained. Tysseling-Mattiace *et al.* (43) reported that injection of amphiphile peptide conjugated IKVAV peptide (mimicking laminin structure supports of the neural ECM), into the injured spinal cord, effectively improved functional recovery after spinal cord injury, in two different injury models (contusion and compression of rat and mouse spinal cord).

Previous studies also have provided evidence for IKVAV-grafted scaffolds promoting bone marrow mesenchymal stem cell (BMMSC) survival and growth in non-degradable PEG hydrogels (44), HA-based hydrogels (45), RGDSP-modified PEG gels (46) and PHEMA scaffolds (47). Results demonstrated that cell numbers and adhesion areas on IKVAV-grafted scaffolds was highest. However, molecular mechanisms of BMMSC behaviour, such as in the cell cycle, apoptosis, cell population growth and proliferation, mediated by IKVAV-grafted scaffolds, has up to now remained a challenge. Thus, to elucidate the mechanism clearly, it is

essential that activities of signal transduction in IKVAV-induced BMMSC proliferation should be studied first.

As a component of the mitogen-activated protein kinase (MAPK) cascade, ERK can be activated by extracellular or intracellular factors. The ERK signalling module consists of two isoenzymes, ERK-1 and -2. Activated ERK-1 and -2 are translocated into nuclei and increase transcriptional activity of genes relevant to cell proliferation (48,49). Akt phosphorylation mediated by phosphatidylinositol 3-kinase (PI3K) in response to various growth/survival factors and activation of the pathway is crucial for regulation of cell survival and apoptosis (50,51). Both PI3K/Akt and MAPK/ERK1/2 signalling pathways are pivotal in cell survival and proliferation (52,53). Survival, migration and proliferation of MSCs are also enhanced by activation of ERK1/2 and PI3K-Akt signalling pathways (54,55).

According to the lines of evidence mentioned above, we hypothesized that IKVAV peptide could affect activities of BMMSC. This study was thus undertaken to determine how IKVAV induces BMMSC population growth and proliferation and roles MAPK/ERK1/2 and PI3K/Akt signalling pathways play in IKVAV-induced BMMSC. Analyses of CCK-8, RT-PCR, western blotting and flow cytometric (FCM) were carried out to explore mechanisms responsible for these effects. Our results indicated that, after treatment with IKVAV peptide, cell viability was higher in a dose- and time-department manner; proliferating cell nuclear antigen (PCNA) mRNA synthesis was up-regulated, cell cycles were activated for them to enter S from G_0/G_1, and Akt and ERK1/2 signalling pathways were activated. The results suggest that IKVAV peptide regulated BMMSC growth and proliferation at the molecular level. To the best of our knowledge, this is the first report on molecular mechanisms of growth and proliferation of BMMSCs induced by IKVAV peptide. Hopefully, the outcome will provide experimental evidence for application of IKVAV-grafted scaffolds in BMMSC-based tissue engineering fields.

Materials and methods

Reagents and instrumentation

Foetal bovine serum (Gibco BRL, Grand Island, NY, USA), αMEM (Hyclone, Logan, UT, USA), 25-cm^2 plastic flasks (Corning, Williamsburg, NY, USA), 96-well plates (Costar, Milpitas, CA, USA), 6-well plates (NUNC, Roskilde, Denmark), trypsin (Hyclone), penicillin/streptomycin (Hyclone), cell counting kit-8 (Beyotime, Haimen, China), annexin V-FITC apoptosis detection kit (BD, San Jose, CA, USA), Trizol Reagent (Invitrogen Life Technologies, NY, USA), TOYOBO THUNDERBIRD SYBR qPCR Mix and TOYOBO First Strand cDNA Synthesis Kit (Toyobo, Shanghai, China), Primers synthesis company (Invitrogen Biotechnology Co., LTD, Carlsbad, CA, USA), marker (10–170 kDa, sm0671; Fermentas, St. Leon-Rot, Germany), Akt (EPI, Burlingame, CA, USA), p-Akt (EPI), ERK1/2 (Bioword Technology, Minnesota, MN, USA), p-ERK1/2 (Bioword), PD98059 (Santa Cruz, Dallas, TX, USA), Wortmannin (Sigma, St. Louis, MO, USA), Revert Aid First Strand cDNA Synthesis Kit (Fermentas, St. Leon-Rot, Germany) Bradford Protein Assay Kit (Beyotime). IKVAV peptides were synthesized by our group. Inverted fluorescence microscopy (IX71; Olympus, Japan). A phase contrast microscope (Olympus, Tokyo, Japan), ELISA (Multiskan Mk3, Thermo Labsystems, Helsinki, Finland) and flow cytometery apparatus (Becton Dickinson, Heidelberg, Germany) were used in the experiments.

Cell isolation and culture

BMMSCs were isolated and identified as reported in our previous work (56); passage 3–5 cells were employed here. Cells were cultured in 25-cm^2 plastic flasks at $2 \times 10^5/cm^2$ at 37 °C in humidified atmosphere of 95% oxygen and 5% carbon dioxide. Cells were cultured in alpha modified Eagle's medium (αMEM) supplemented with 10% FBS, 2 mM L-glutamine, 100 U/ml penicillin, 100 μg/ml streptomycin and 3.7 g/l $NaHCO_3$. Culture medium was replaced with fresh medium every 3 days. Cells were detached with 0.25% trypsin containing 0.02% ethylene diamine tetraacetic acid when incubated to 90% confluence.

Synthesis and characterization of IKVAV peptides

IKVAV peptides were synthesized using a Discover solid-phase automated synthesizer. Two grams Fmoc-Val-wang resin was soaked in 10 ml DMF solution for 1 h. Subsequently, Fmoc groups on the Fmoc-Val-wang resin mixture were eluted with DMF solution supplemented with 20% piperidine. Amino acid/PyBOP/HOBT/DIEA active solution was respectively prepared and put into the peptide synthesizer for amino acid condensation reaction. 6% ninhydrin ethanol solution with little resin was heated at 100 °C for 2 min. All above steps were repeated. Acrylic acid was added up to the end of the peptide chain. Reagent (TFA/TIPS/water = 95/2.5/2.5) was used to cleave peptides from the resin by stirring for 2 h at room temperature. After washing in TFA, filtrate was collected and added into cold ether and precipitated peptides were produced; crude peptides were then collected and vacuum dried. Peptides were obtained after processing, purification and freeze dehydration. All peptides were

synthesized in the amide acid form. Composition and purity of peptides were determined by amino acid analysis and high-performance liquid chromatography. Small samples were taken for high-performance liquid chromatography and mass spectroscopy. Properties of IKVAV peptide have been shown in our previous work (57).

Cell viability assay

Cell viability was examined using CCK-8 assay. BMMSC (5×10^4/well) were cultured in 96-well plates with αMEM medium containing 8% FBS. Twenty-four hours later, medium was replaced with αMEM containing IKVAV or PBS (control group); treated period ranged from 0 to 72 h. Concentration gradient of IKVAV in medium ranged from 0.004 to 2.5 mM. For quantitative analysis of cell proliferation, 10 μl WST-8 solution was added to each well. After the given treatment period, absorbance at 450 nm was monitored by ELISA. Cell proliferation was calculated by normalizing optical densities (OD) to those of control cells incubated in PBS.

Flow cytometry analysis

Cell cycle and apoptosis of BMMSC treated with IKVAV were determined by FCM analysis. Apoptosis was revealed using an annexin V-FITC apoptosis detection kit according to the manufacturer's protocol. BMMSCs were cultured at 6×10^5 cells/ml in 6-well plates, in αMEM containing IKVAV of various concentrations or PBS (control group) for 24 h. Cells were harvested by trypsinization, then washed twice in cold PBS then centrifuged at 700 ***g***. In the region of 1×10^5 to 1×10^6 cells were resuspended in 500 μl binding buffer, centrifuged again at 1000 rpm for 5 min before the supernatant being removed.

For cell cycle assay, −20 °C pre-cooled 90% ethanol was added slowly to the cells, which were then resuspended and kept overnight in an ice bath. Cells were centrifuged again at 1000 rpm for 5 min and supernatant was removed. They were resuspended in 250 μl PBS with 2 μl RNaseA (1 mg/ml in deionized water) and kept in a 37 °C water bath for 40 min; 50 μl PI (100 μg/ml in PBS) was added and cells were stained in the dark for 20 min. The cell cycle was examined at 488 nm by flow cytometry and cell cycle proration was analysed by Cell Quest (BD Biosciences, San Jose, CA, USA) and Modfit software (BD Biosciences).

For the assay of apoptosis, cells were resuspended in 500 μl binding buffer and transferred to a sterile flow cytometry glass tube. Five microlitres of annexin V-FITC and 5 μl propidium iodide were added then incubated in the dark for 10 min, at room temperature. Cells were analysed by flow cytometry at 488 and 530 nm. Distribution of cells was analysed using Cell Quest™ software in the flow cytometer within 1 h of staining. Data from 10 000 cells were collected for each data file. Apoptotic cells were identified as being annexin V-FITC-positive and PI-negative.

Real-time fluorescence quantitative polymerase chain reaction

Total cell mRNA was extracted from IKVAV-induced BMMSC using Trizol reagent, according to the manufacturer's instructions. Isolated RNA was stored at −70 °C in diethylpyrocarbonate (DEPC)-treated water, and quantity and quality of RNA were determined by absorbance of SYBR green II fluorescent dye at 260/280 nm. Total RNA was reverse transcribed into complementary DNA (cDNA) using Revert Aid First Strand cDNA Synthesis Kit (Creative Biogene, Shirley, NY, USA) according to the manufacturer's instructions. Primer sequences used in this context are listed as follows: PCNA primers: sense, TTTCACAAAAGCCACTCCACTG; antisense, CTTT AAGTGTCCCATGTCAGCAAT. GAPDH was used as internal control and detected using the following primers: sense, CGCTAACATCAAATGGGGTG; antisense, TTG CTGACAATCTTGAGGGAG. Polymerase chain reaction (PCR) amplification was performed with the following parameters: 40 amplification cycles for PCNA and GAPDH (95 °C for 1 min, at 58 °C for 45 s, 72 °C for 20 s). Gene expression was presented using a modification of the $2^{-\Delta\Delta Ct}$ method.

Western blot analysis

BMMSCs were treated with IKVAV at different concentrations in the presence or absence of kinase inhibitors, as indicated for a variety of time periods. Cells were treated with lysis buffer (1 mM phenylmethylsulphonylfluoride was added before using). Lysates were subsequently centrifuged at 12 000 ***g*** for 5 min and supernatant was collected for protein analysis; sample protein concentration was determined using the Bradford Protein Assay Kit (Beyotime Institute of Biotechnology, Haimen, China). Equal amounts of protein from cell lysates were first resuspended in sample buffer containing 62 mM Tris-HCl (pH 6.8), 2% sodium dodecylsulphate, 10% glycerol, 5% β-mercaptoethanol and 0.04% bromphenol blue, then resolved by sodium dodecylsulphate-polyacrylamide gel electrophoresis and transferred to polyvinylidene difluoride membranes. After brief washing in Tris-buffered saline Tween-20 (TBST) (25 mM Tris-HCl (pH 7.5), 50 mM NaCl, 0.1% Tween-20), membranes were blocked with 5% (in TBST)

skimmed dried milk for 1 h. Membranes were incubated overnight at 4 °C with the appropriate concentration of primary antibody. After washing in TBST, membranes were incubated in secondary antibody for 30 min, washed again in TBST and left on a shaking table. Blots were detected using an ECL kit, and signals were quantified by scanning densitometry. All data were expressed as relative differences between control and treated cells after normalization to GAPDH expression. In addition, PD98059 and wortmannin were employed to inhibit MAPK/ERK1/2 and PI3K/Akt signals in the experiment. BMMSCs were pretreated with the appropriate inhibitor for 30 min then the IKVAV was added. Western blot analysis was performed 24 h following IKVAV treatment.

Statistical analysis

All experiments were performed in triplicate and analysed using statistical software SPSS 13.0 (SPSS Inc., Chicago, IL, USA). Analysis results were expressed as mean ± SD and $P \leq 0.05$ were considered significant.

Results

PCNA expression of IKVAV-induced BMMSCs

To investigate the effect of IKVAV on cell proliferation, BMMSCs were cultured with different concentrations of IKVAV (0, 0.004, 0.02, 0.1, 0.5 and 2.5 mM) for 48 h. PCNA expression level of IKVAV-treated BMMSC was tested by real-time fluorescence quantitative PCR, and PCNA of different cell cycle phases was determined by enumerating distribution of double-stranded DNA. Results showed that PCNA synthesis stimulated by IKVAV was dose- and time-dependent. PCNA expression increased to 2.2 times more than that of controls when density peaked at 0.5 mM, then decreased (Fig. 1a). PCNA synthesis decreased with increasing incubation time and peaked at 12 h; at that time, it was 8 greater than that of the control group. It then started to decline (Fig. 1b).

Effects of IKVAV on BMMSC cell cycle phase distribution

To clarify the influence of IKVAV on the BMMSC cell cycle, cell cycle distribution was determined by flow cytometry. Flow cytometric analysis in Table 1 shows that compared to the control group, distribution of cells in G_0/G_1 of the IKVAV-treated group attenuated gradually by density and declined significantly in the 0.5 mM group ($*P < 0.05$). Meanwhile, distribution of S phase cells was elevated by IKVAV density and peaked at 0.5 mM ($**P < 0.01$). Distribution of G_2/M phase cells did not change to any noticeable extent. Maximum response of S phase cells of IKVAV-treated BMMSC appeared at 0.5 mM, in which it was 4.2 times greater than the control group; phase distributions of G_0/G_1 and G_2/M cells declined correspondingly (Fig. 2, $*P < 0.05$). These results demonstrate that IKVAV acted as a signalling molecule, inducing the BMMSC cell cycle for cells to enter S phase from G_0/G_1 and arrested them from entering G_2/M phase; the increased proportion of S phase in cell cycle was considered to be a sign of BMMSC proliferation. IKVAV at 0.5 mM was the most suitable concentration for BMMSC population growth.

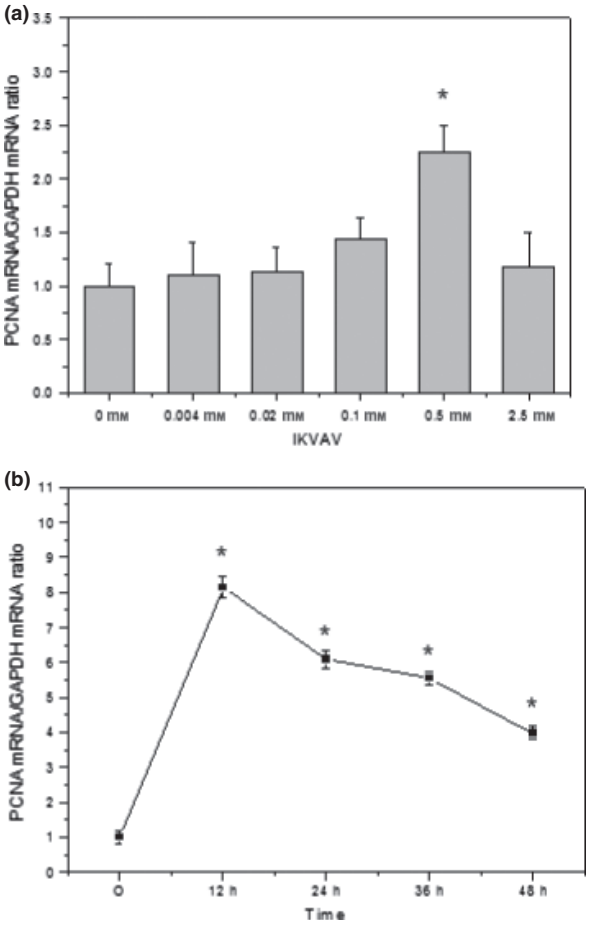

Figure 1. PCNA expression in IKVAV-induced BMMSCs. The biosynthesis of PCNA mRNA was in a concentration- (a) and time- (b) dependent manner. Experiments were performed at least in triplicate ($*P < 0.05$).

Effects of IKVAV on BMMSC viability

Effects of IKVAV at various concentrations (0, 0.004, 0.02, 0.1, 0.5 and 2.5 mM) treating BMMSC for different time intervals (0, 24, 48, 72 h) on their viability were determined by CCK-8 assay. OD values were

tested every 24 h for 72 h after co-culture. As shown in Fig. 3a, cell viability increased gradually at concentrations from 0 to 0.5 mM, peaked at 0.5 mM and then declined. Highest OD value was observed at 72 h when treated with IKVAV at 0.5 mM (Fig. 3b) (*$P < 0.05$). These results demonstrated that IKVAV promoted BMMSC proliferation in a dose- and time-dependent manner. Apoptosis was tested for by FCM analysis of annexin V FITC/propidium iodide (PI) staining of BMMSC treated with IKVAV at 0.5 mM, after 24 h. Figure 3c and 3d indicate that there was no clear reduction in live cell percentage in the IKVAV-treated group (93.25%) compared to the control group (94.34%). Only a low apoptotic fraction was observed after 24-h treatment. Apoptotic level of the 0.5 mM IKVAV-treated group (2.37%) was almost the same as that of the control group (2.35%).

Table 1. Effects of IKVAV on the cycle phase distribution of BMMSC

	Cycle phase distribution (%)		
Concentration of IKVAV	G_0/G_1	S	G_2/M
0 mM	92.943 ± 0.987#	2.047 ± 1.104&	5.014 ± 0.788
0.004 mM	92.167 ± 1.033#	2.325 ± 1.015&	5.513 ± 0.547
0.02 mM	91.563 ± 0.905#	2.720 ± 0.845&	5.721 ± 0.731
0.1 mM	91.873 ± 0.196#	2.518 ± 0.712&	5.612 ± 0.753
0.5 mM	84.743 ± 1.644*	10.577 ± 1.272**	4.677 ± 1.048*
2.5 mM	92.103 ± 1.365#	2.202 ± 0.947&	5.703 ± 1.035

Compared with the group of 0 mM, *$P < 0.05$, **$P < 0.01$; Compared with the group of 0.5 mM, #$P < 0.05$, &$P < 0.05$; $N = 3$.

Activation of ERK1/2 and Akt in IKVAV-induced BMMSC

Activation of ERK1/2 and Akt has been reported to play an important role in regulation of cell survival and proliferation (32,38–40). Here, two signalling pathways were monitored by measuring phosphorylation levels of ERK1/2 and Akt, in IKVAV-treated BMMSC. Western blot analysis was used to determine activities of Akt, ERK1/2, phosphorylated-Akt (p-Akt), and phosphorylated-ERK1/2 (p-ERK1/2) in total protein, extracted from BMMSC at the end of co-culture. As shown in Fig. 4, levels of p-ERK1/2 and p-Akt increased significantly in a dose- and time-dependent manner after IKVAV treatment. As shown in Fig. 4a and 4b, gradually increased levels of p-ERK1/2 and p-Akt were observed with increase in IKVAV concentration. Maximum response appeared at 0.5 mM, then a decline followed. Levels of p-ERK1/2 and p-Akt were 2.1 and 7 times greater than those of the control group (*$P < 0.05$), respectively. There were fewer responses of p-ERK1/2 and p-Akt with 2.5 mM IKVAV-treated BMMSC than with 0.1 and 0.5 mM. However, remark-

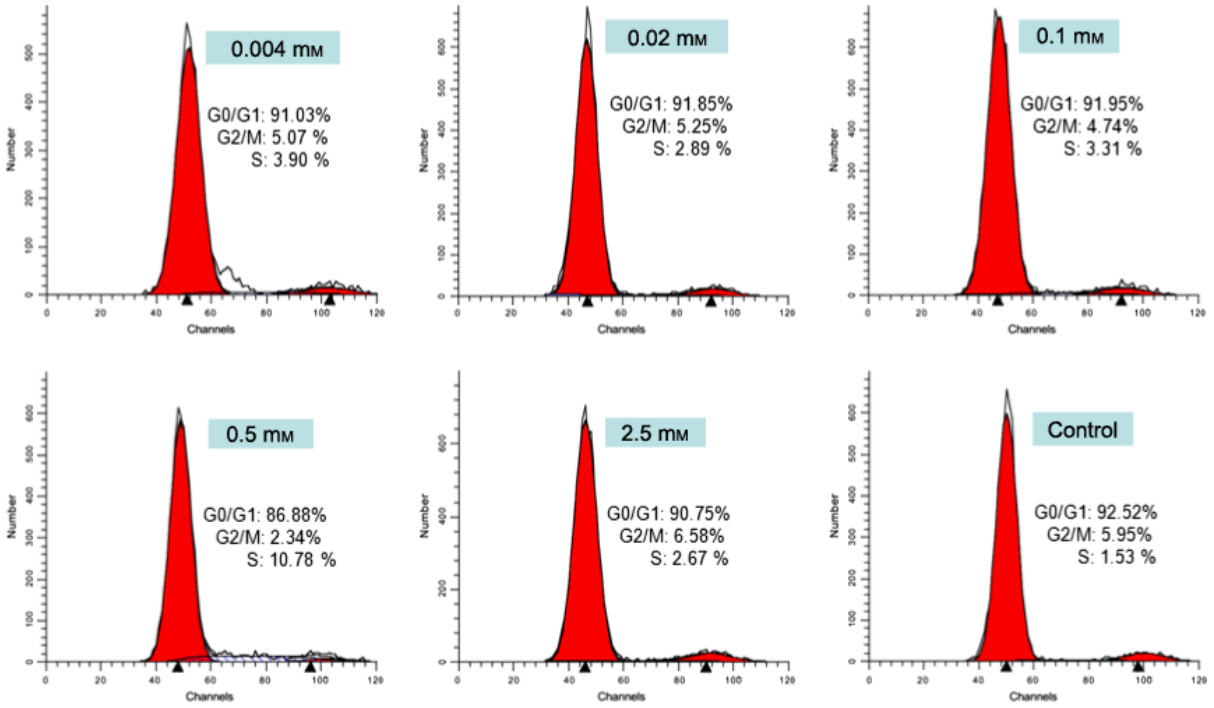

Figure 2. Effect on cell cycle of IKVAV-induced BMMSC. Flow cytometry of cell cycle analysis in various concentrations of IKVAV (0, 0.004, 0.02, 0.1, 0.5 and 2.5 mM). Experiments were performed at least in triplicate (*$P < 0.05$).

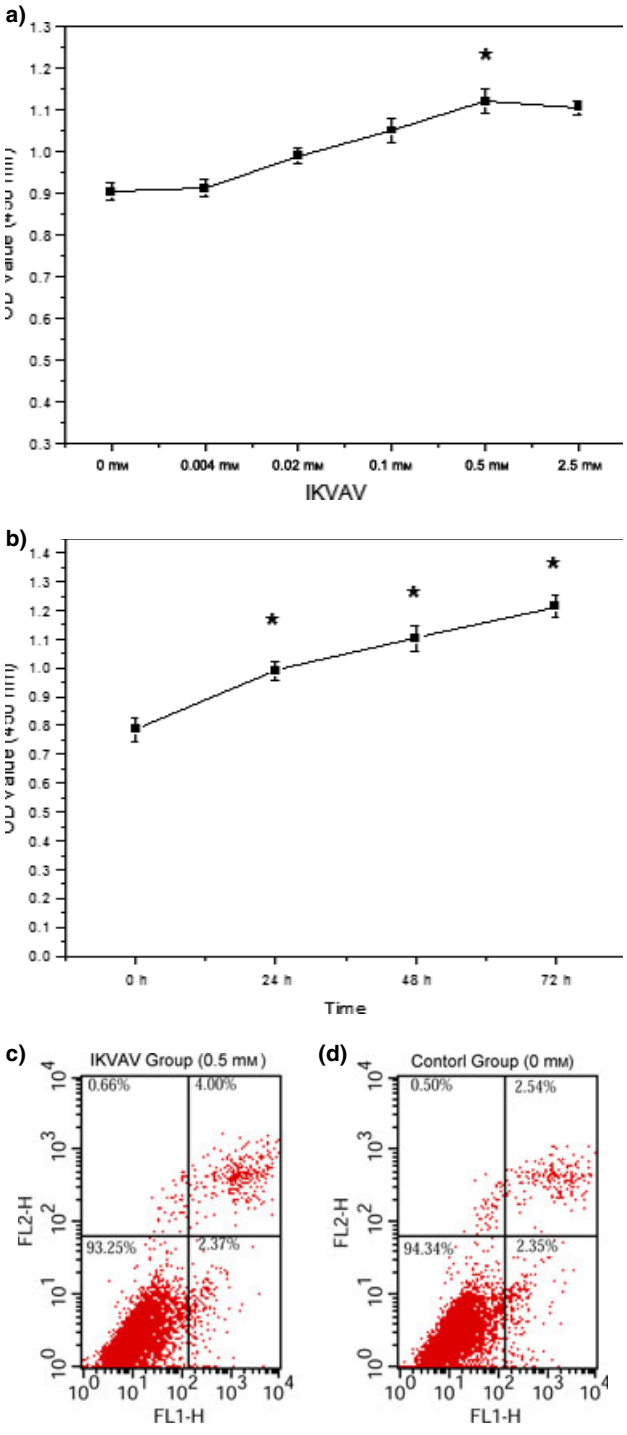

Figure 3. Effects of IKVAV on viability and apoptosis of BMMSC. Cell proliferation status was detected by CKK-8 assay. Cells were treated with different concentrations of IKVAV for the indicated time in 72 h. IKVAV promoted cell proliferation in a dose- (a) and time- (b) dependent manner. Cell apoptosis induced by IKVAV was detected by flow cytometric analysis. Cell apoptosis has no significant difference between the 0.5 mM IKVAV-treated group (c) than that of the control group (d). Experiments were performed at least in triplicate (*$P < 0.05$).

able phosphorylation of ERK1/2 and Akt in BMMSCs treated with 0.5 mM IKVAV was observed after 24 h. Data from Fig. 4c and 4d show that BMMSCs treated with IKVAV for 24 h significantly increased levels of p-ERK (22-fold) and p-Akt (5-fold) compared to the control group (*$P < 0.05$).

Inhibition of proliferation of IKVAV-induced BMMSCs by inactivation of MAPK/ERK and PI3K/Akt signalling pathways

To determine roles of ERK1/2 and Akt signalling pathways activated by IKVAV treatment, MAPK/ERK pathway inhibitor PD98059 and PI3K/Akt pathway inhibitor wortmannin were utilized (58,59). An clear reduction in p-Akt and p-ERK expression was observed after pre-treatment with wortmannin and PD98059 according to western blot analysis. As shown in Fig. 5, IKVAV-induced p-ERK1/2 activation was reduced by 23.86% in cells pre-treated with PD98059 at 10 μM compared to the untreated group (Fig. 5a). While IKVAV-induced p-Akt activation was reduced by 17.61% in BMMSCs pre-treated with wortmannin at 100 nM compared to the untreated group (Fig. 5b). These results indicate that treating BMMSC with 10 μM PD98059 and 100 nM wortmannin effectively blocked the enhanced proliferation of IKVAV-induced BMMSCs.

RT-PCR was used to test mRNA synthesis of PCNA in BMMSC pre-treated with the inhibitors. Results in Fig. 6 show that PCNA expression was reduced to 27.14% by PD98059 compared to the untreated group, to 51.49% by wortmannin, and to 77.99% by simultaneous use of both inhibitors. Furthermore, expressions of PCNA mRNA were significantly different when comparing IKVAV-induced BMMSCs with the control group (*$P < 0.05$), PD98059-treated group (*$P < 0.05$) and the wortmannin-treated group (*$P < 0.05$).

In addition, there were significant differences in percentage of proliferating cells comparing IKVAV-treated BMMSC with the control group (**$P < 0.01$), PD98059-treated group (*$P < 0.05$), the wortmannin-treated group (*$P < 0.05$) and the combined treatment group. As showed in Fig. 7, CCK-8 analysis demonstrated that the effect of IKVAV on BMMSs viability was partly reduced by 10.71, 35.65 and 50.25% when treated with PD98059, wortmannin, and the combination treatment, respectively.

Discussion

In this work, molecular mechanisms of IKVAV-induced BMMSC population growth and proliferation were studied. We focused mainly on roles of ERK1/2

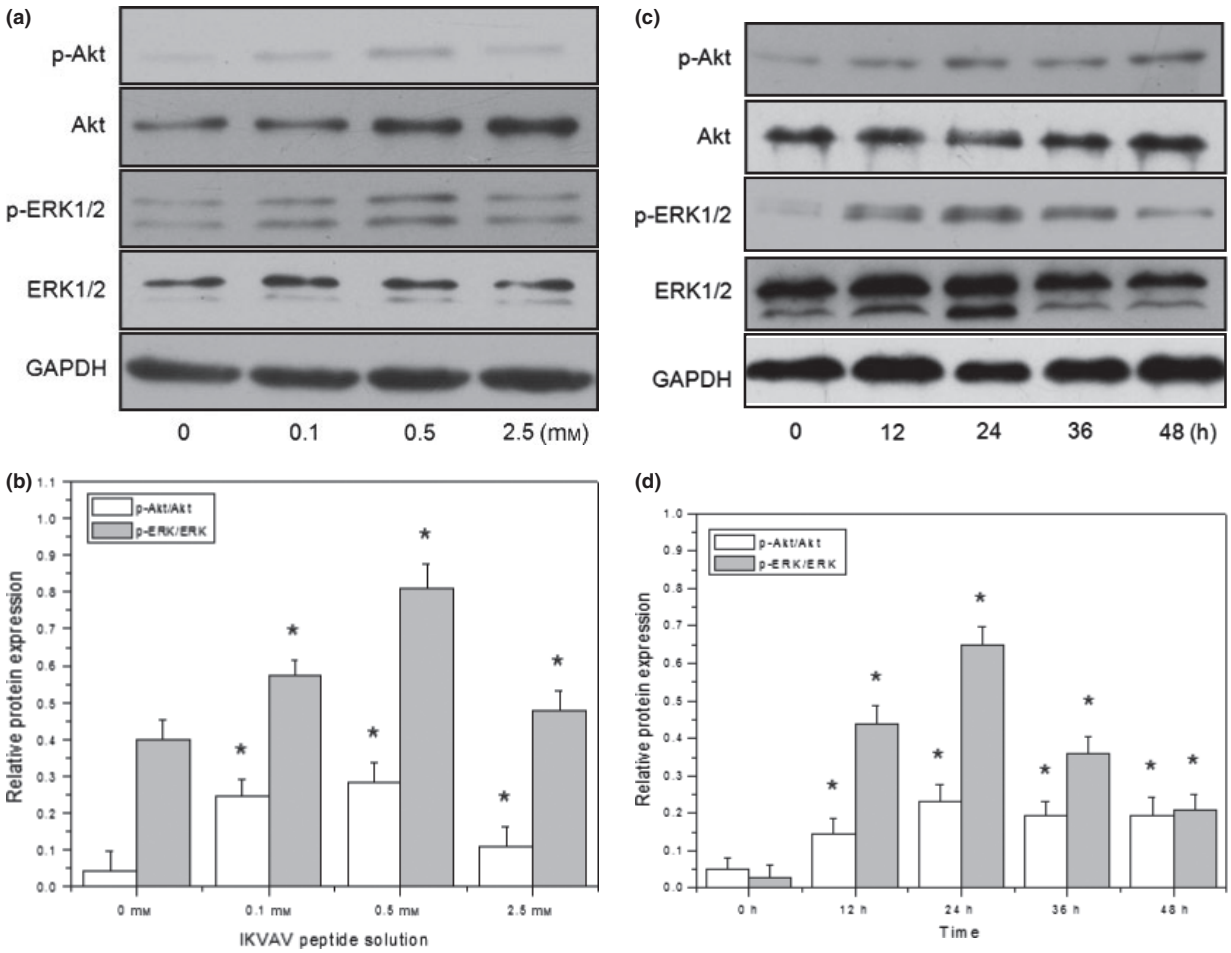

Figure 4. Analysis of IKVAV-induced phosphorylation levels of ERK1/2 and Akt in BMMSCs by western blot. Total proteins of BMMSCs treated with different concentrations (IKVAV-untreated as control group) of IKVAV for various times (treated by 0 h as control) were used for detection by western blot for their phosphorylated and unphosphorylated ERK1/2 and Akt. The ERK1/2 and Akt signaling pathways were activated by IKVAV in a dose- (a, b) and concentration- (c, d) dependent manner. Experiments were performed at least in triplicate (*$P < 0.05$).

and Akt kinase cascades activated by IKVAV. When the IKVAV-induced BMMSC were respectively pre-treated with inhibitors PD98059 and wortmannin, activities of p-ERK1/2 and p-Akt decreased significantly. These results suggest that both signalling pathways play important roles in the growth and proliferation of BMMSC treated with IKVAV peptide.

As the active sequence of laminin, IKVAV has been identified as capable of mimicking some biological activities of intact molecules for cell attachment, migration and growth (26,60). IKVAVA peptides can be absorbed and used directly by an organism (61). Degradation of IKVAV peptides is enzymatic *in vivo* and by proteolysis *in vitro*. Degradation products are of low molecular weight non-toxic amino acids, which are easily absorbed and metabolized by the organism. However, whether the degradation products can affect cell activities or how they might influence types of cell behaviour have not previously been reported. Due to superior biological activities of IKVAV peptide, it has been widely used in tissue engineering by immobilizing it on to hydrogel scaffolds (62–64). IKVAV thus grafted, effectively binds to cell membrane integrin receptors, and thus mediates interaction with the cell surface (65). In previous studies, IKVAV-modified hydrogels have been proven to promote adhesion, growth and proliferation of neural stem cells (19,47), and neuron (66,67) adhesion, growth and proliferation *in vitro*. In implantation assays, IKVAV peptide-grafted scaffolds have been shown to enhance regenerative function of brain (68) and spinal cord (69) cells.

Recently, adhesion, morphology, growth and proliferation of MSCs have been investigated on IKVAV-modified hydrogels, such as PHEMA (47), PEG (44) and nanofibre gel (70). IKVAV-modified porous scaffolds significantly increased numbers of attached cells

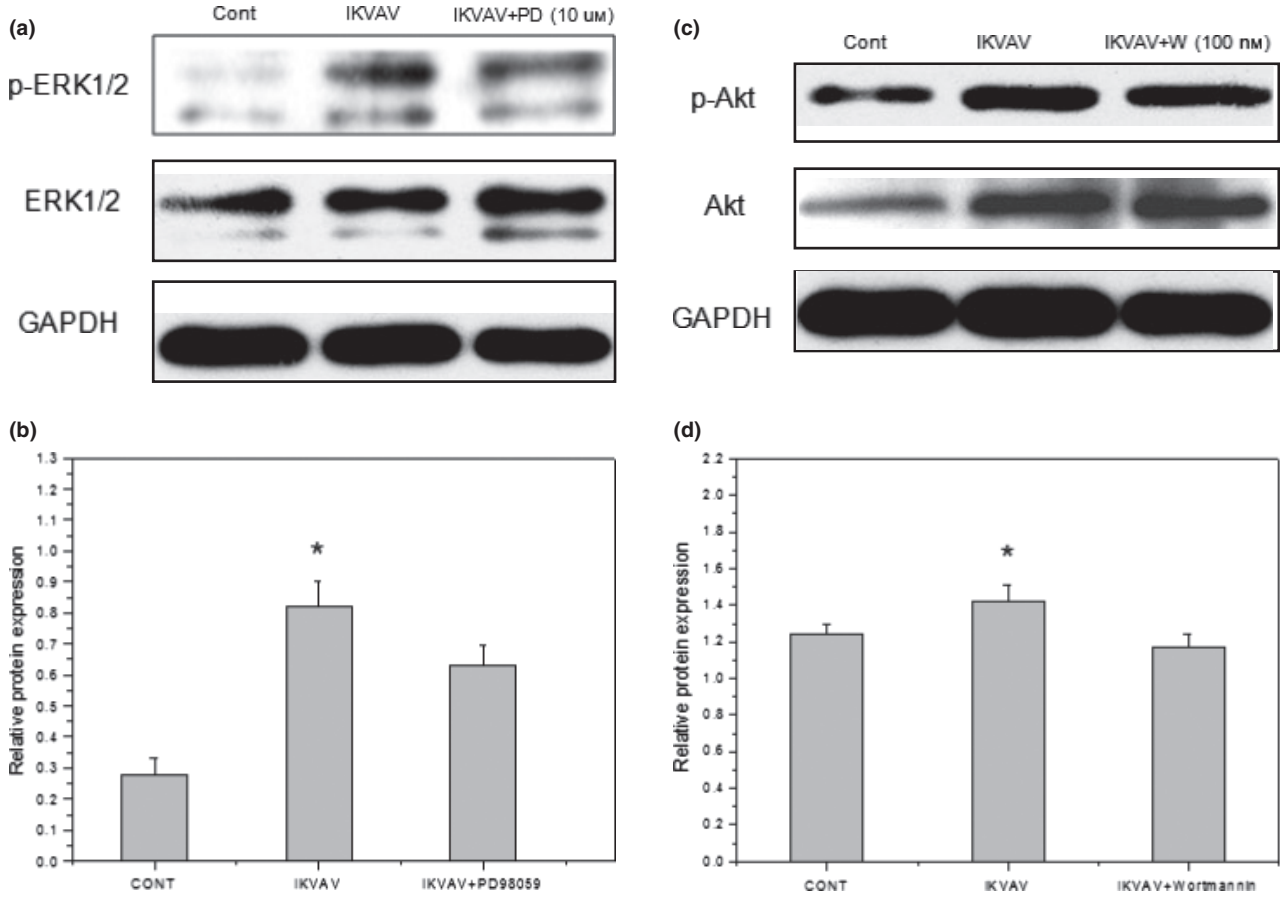

Figure 5. Inhibition evaluation of IKVAV-induced phosphorylation levels of ERK1/2 and Akt by inhibitors of ERK1/2 and Akt signaling pathways in BMMSCs. BMMSCs were treated with 0.5 mM IKVAV after pretreatment of PD98059 (10 μM) or wortmannin (100 nM). Cell extracts were prepared at the end of 24 h co-culture, then p-ERK1/2, p-Akt and total ERK, Akt were determined by western blot analysis. Experiments were performed at least in triplicate (*$P < 0.05$).

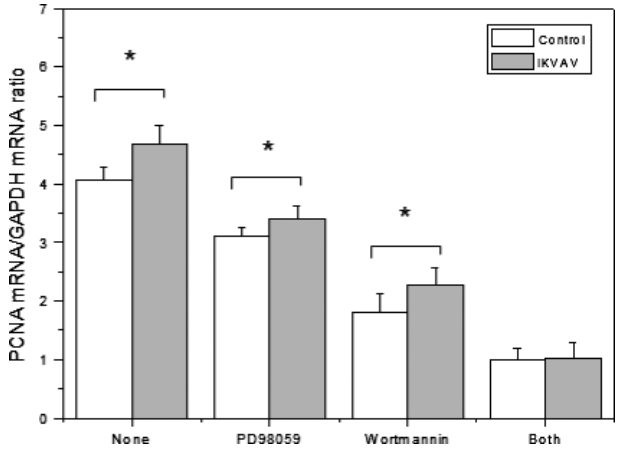

Figure 6. Effects of two inhibitors on PCNA synthesis of IKVAV-induced BMMSCs. BMMSCs were pretreated by PD98059 (10 μM) or wortmannin (100 nM) or both of them, then stimulated by 0.5 mM IKVAV. The expression of PCNA was detected by RT-PCR. Experiments were performed at least in triplicate (*$P < 0.05$).

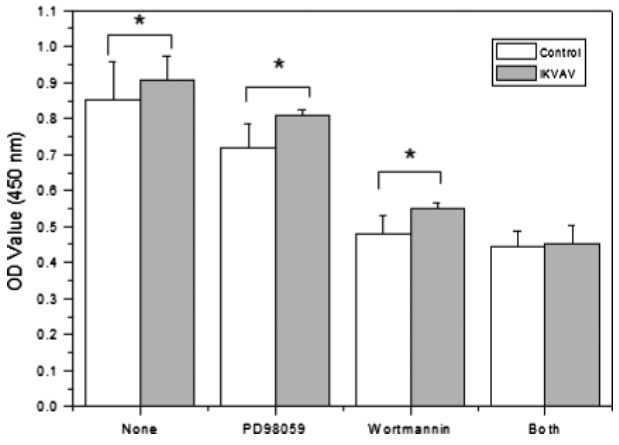

Figure 7. Proliferation of BMMSCs interacting with two inhibitors (PD98059 and wortmannin). Cell viability was detected by CCK-8 assay at 24 h. Experiments were performed at least in triplicate (*$P < 0.05$).

and enhanced their viability on the hydrogel surface. In those studies, cell proliferation was determined by counting live cells on the scaffolds under fluorescence microscope/laser confocal microscopy, or cell viability by CCK-8/MTT assay. However, precise molecular mechanisms that induced cell proliferation were not completely proven. IKVAV is a bioactive peptide whose effects on change of cell morphology and growth status remain unclear, including interaction of bioactivators and transduction of signal molecules. IKVAV peptide has been previously proven to enhance MSC adhesion and proliferation at the cellular level, but few studies have illustrated molecular mechanisms.

To illustrate cell population growth and proliferation mechanisms, we investigated effects of IKVAV peptide on BMMSC proliferation at cellular and molecular levels. CCK-8 assays indicated that cell viability gradually increased in a dose- and time-dependent manner after IKVAV treatment (Fig. 3a,b). Viability of BMMSCs treated with IKVAV at 0.5 mM after 24 h was 22.3% higher than the control group, and 53.8% higher after 72 h than the control group. Cell proliferation was clearly promoted by treatment with IKVAV. Although viability was enhanced, amounts of dead cells did not increase overtly compared to the control group during incubation (Fig. 3c,d). Levels of apoptosis in the IKVAV-treated group and the control group were 2.37% and 2.35%, which were lower than that in human BMMSCs (3.7%) (71), indicating that IKVAV did not induce apoptosis. FCM analysis of the cell cycles demonstrated that cells in G_0/G_1 and S phases of the cell cycle were activated and their proportions ascended markedly when treated with IKVAV in 0.5 mM medium for 24 h. IKVAV peptide might possibly have the function of regulating gene expression associated with proteins controlling cell proliferation. In advance of DNA replication initiation, PCNA is bound to potential start points of DNA replication and relative enzymes; DNA polymerase α and δ are essential for DNA replication in the nucleus. Activity of DNA polymerase δ is markedly enhanced by PCNA, which is expressed only in proliferative cells as they cycle (72). So, expression of PCNA was investigated here by RT-PCR. PCNA expression is committed to DNA synthesis and is widely used as a marker of cell proliferation (73). Cells duplicate their entire genome during S phase of the cell cycle, and the cell cycle processes continuously. RT-PCR results here demonstrated that expression of PCNA in IKVAV-treated BMMSCs was increased in a dose- and time-dependent manner (Fig. 1). According to these results, we concluded that some proliferation-related signalling pathways must have taken part in the cell cycle and regulated the progress of proliferation (74–77). To explore whether proliferation-related signalling pathways were activated, expression of p-Akt, Akt and p-ERK1/2, ERK1/2 were detected every 12 h for 48 h by western blotting. Results demonstrated that activities of p-ERK1/2 and p-Akt increased significantly in a dose- and time-dependent manner after IKVAV treatment (Fig. 4a,b). Population growth and proliferation of IKVAV-treated BMMSCs were mediated by enhancing phosphorylation levels of ERK1/2 and Akt.

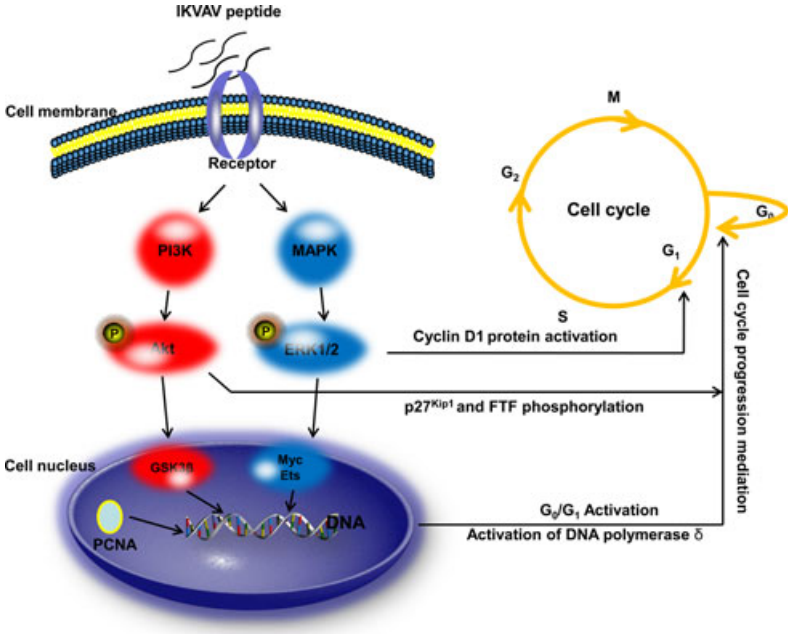

Figure 8. The mechanism figure of IKVAV induces BMMSC growth and proliferation. The IKVAV peptide recognizes and binds to a cell surface protein, and then this IKVAV-binding protein activates the phosphorylation of Akt and ERK1/2. ERK1/2 activation plays a fundamental role for G_1/S transition, because its activation is the trigger for the induction of the cyclin D1 protein, and the down-regulation of several anti-proliferative genes during the G_1 phase. Akt mediates cell cycle progression by phosphorylation of $p27^{Kip1}$ and forkhead transcription factor. This leads to the activation of DNA polymerase α and δ. The activity of DNA polymerase δ is markedly enhanced by PCNA, which is only expressed in proliferating cells. With the proportion of S increased gradually, the cell cycle goes into the S phase from the G_0/G_1 phase. Cell growth and proliferation was promoted finally.

To the best of our knowledge, this is the first study to discover the role of ERK1/2 and Akt signalling pathways during proliferation of BMMSCs induced by IKVAV peptide. Activation of phosphoinositol-3 kinase (PI3K)/Akt pathway leads to cell cycle progression through G_0/G_1 and entry into the S phase. The ERK1/2 signalling pathway is a further signal regulation associated with cell cycle progression, and promotion of cell survival and proliferation (78,79). Our results reveal that, compared to the control group, IKVAV-treated BMMSCs had larger proportions of S phase cells, higher viability, PCNA expression and phosphorylation level of ERK1/2 and Akt. This means that BMMSCs were induced to enter S phase from G_0/G_1; meanwhile, expression of PCNA was enhanced, and phosphorylation of ERK1/2 and Akt were activated. These lines of evidence demonstrate that IKVAV-induced BMMSC growth and proliferation are regulated by ERK1/2 and Akt signalling pathways.

The signalling mechanism might be as follows: IKVAV peptide recognizes and binds to a cell surface protein, which subsequently activates phosphorylation of Akt and ERK1/2; ERK1/2 activation plays a fundamental role on G_1/S transition, as its activation is the trigger for induction of cyclin D1 protein, and down-regulation of several anti-proliferative genes during the G_1 phase (80). Akt mediates cell cycle progression by phosphorylation of $p27^{Kip1}$ (81) and forkhead transcription factor (82). This leads to activation of DNA polymerases α and δ; activity of DNA polymerase δ is markedly enhanced by PCNA, which is expressed in proliferating cells only. With the gradually increasing proportion of S phase cells, they enter S phase from G_0/G_1 phase (83,84); cell population growth and proliferation are finally promoted (Fig. 8).

To examine whether activation of the above two signalling pathways, which mediated BMMSC proliferation by IKVAV, was functionally involved in phosphorylation of ERK1/2 and Akt, the ERK1/2 and Akt signalling pathway inhibitors PD98059 and wortmannin were employed. Under treatment of inhibitors, p-ERK1/2 and p-Akt levels were both down-regulated, and PCNA expression and cell viability were reduced, correspondingly. Therefore, we concluded that both PCNA mRNA biosynthesis of PCNA and proliferation activities of IKVAV-induced BMMSCs were regulated by MAPK/ERK1/2 and PI3K/Akt signalling pathways. Our results indicate that inactivation of Akt and ERK1/2 signalling pathways clearly suppressed IKVAV-induced BMMSC growth and proliferation. Akt and ERK1/2 signalling pathways play an important role in IKVAV-induced BMMSC population growth and proliferation.

In summary, we identified the role of IKVAV peptide in regulation of BMMSC population growth and proliferation through activating Akt and ERK1/2 signalling pathways. These results demonstrate that IKVAV peptide stimulated activation of MAPK/ERK1/2 and PI3K/Akt cascades, and promoted mRNA biosynthesis of PCNA and proliferation of BMMSC. This is the first study to point out the modulation function of IKVAV peptide on BMMSC growth and proliferation at the signal transduction level. This outcome provides experimental evidence for the application of IKVAV-grafted scaffolds in the BMMSC-based tissue engineering field.

Acknowledgements

This work was supported by the State Basic Research Foundation of China (2011CB606205), Self-determined and Innovative Research Funds of Wuhan University of Technology (WUT: 2012-YB-007), the Key Grant Project of Chinese Ministry of Education (313041), the Fundamental Research Funds for the Central Universities (WUT: 2013-IV-047) and the National Natural Science Foundation of China (51103112 and 31300791).

References

1 Caplan AI (1991) Mesenchymal stem cells. *J. Orthop. Res.* **9**, 641–650.
2 Barrilleaux B, Phinney DG, Prockop DJ, O'connor KC (2006) Review: ex vivo engineering of living tissues with adult stem cells. *Tissue Eng.* **12**, 3007–3019.
3 Timper K, Seboek D, Eberhardt M, Linscheid P, Christ-Crain M, Keller U *et al.* (2006) Human adipose tissue-derived mesenchymal stem cells differentiate into insulin, somatostatin, and glucagon expressing cells. *Biochem. Biophys. Res. Commun.* **341**, 1135–1140.
4 Shake JG, Gruber PJ, Baumgartner WA, Senechal G, Meyers J, Redmond JM *et al.* (2002) Mesenchymal stem cell implantation in a swine myocardial infarct model: engraftment and functional effects. *Ann. Thorac. Surg.* **73**, 1919–1926.
5 Toma C, Pittenger MF, Cahill KS, Byrne BJ, Kessler PD (2002) Human mesenchymal stem cells differentiate to a cardiomyocyte phenotype in the adult murine heart. *Circulation* **105**, 93–98.
6 El-Ansary M, Abdel-Aziz I, Mogawer S, Abdel-Hamid S, Hammam O, Teaema S *et al.* (2012) Phase II trial: undifferentiated versus differentiated autologous mesenchymal stem cells transplantation in Egyptian patients with HCV induced liver cirrhosis. *Stem Cell Rev. Rep.* **8**, 972–981.
7 Zhang Z, Lin H, Shi M, Xu R, Fu J, Lv J *et al.* (2012) Human umbilical cord mesenchymal stem cells improve liver function and ascites in decompensated liver cirrhosis patients. *J. Gastroenterol. Hepatol.* **27**(Suppl 2), 112–120.
8 Peng L, Xie DY, Lin BL, Liu J, Zhu HP, Xie C *et al.* (2011) Autologous bone marrow mesenchymal stem cell transplantation in liver failure patients caused by hepatitis B: short-term and long-term outcomes. *Hepatology* **54**, 820–828.
9 Yen TH, Alison MR, Cook HT, Jeffery R, Otto WR, Wright NA *et al.* (2007) The cellular origin and proliferative status of regener-

ating renal parenchyma after mercuric chloride damage and erythropoietin treatment. *Cell Prolif.* **40**, 143–156.
10 Wise AF, Ricardo SD (2012) Mesenchymal stem cells in kidney inflammation and repair. *Nephrology* **17**, 1–10.
11 Le Blanc K, Rasmusson I, Sundberg B, Götherström C, Hassan M, Uzunel M *et al.* (2004) Treatment of severe acute grat-versus-host disease with third party haploidentical mesenchymal stem cells. *Lancet* **363**, 1439–1441.
12 Uccelli A, Moretta L, Pistoia V (2008) Mesenchymal stem cells in health and disease. *Nat. Rev. Immunol.* **8**, 726–736.
13 Griffin M, Iqbal SA, Bayat A (2011) Exploring the application of mesenchymal stem cells in bone repair and regeneration. *J. Bone Joint Surg. Br.* **93**, 427–434.
14 Bruder SP, Kurth AA, Shea M, Hayes WC, Jaiswal N, Kadiyala S (1998) Bone regeneration by implantation of purified, culture-expanded human mesenchymal stem cells. *J. Orthop. Res.* **16**, 155–162.
15 Patel DM, Shah J, Srivastava AS (2013). Therapeutic potential of mesenchymal stem cells in regenerative medicine. *Stem Cells Int.* **2013**, 1–15.
16 Krebsbach PH, Kuznetsov SA, Bianco P, Robey PG (1999) Bone marrow stromal cells: characterization and clinical application. *Crit. Rev. Oral Biol. Med.* **10**, 165–181.
17 Pittenger MF (2010) *Umbilical Cord Blood: A Future for Regenerative Medicine*, pp 89–97. Singapore: World Scientific Publishing Co. Pte. Ltd.
18 Porada CD, Zanjani ED, Almeida-Porada G (2006) Adult mesenchymal stem cells: a pluripotent population with multiple applications. *Curr. Stem Cell Res. Ther.* **1**, 365–369.
19 Silva GA, Czeisler C, Niece KL, Beniash E, Harrington DA, Kessler JA *et al.* (2004) Selective differentiation of neural progenitor cells by high-epitope density nanofibers. *Science* **303**, 1352–1355.
20 Hodgkinson CP, Gomez JA, Mirotsou M, Dzau VJ (2010) Genetic engineering of mesenchymal stem cells and its application in human disease therapy. *Hum. Gene Ther.* **21**, 1513–1526.
21 Elnakish MT, Hassan F, Dakhlallah D, Marsh CB, Alhaider IA, Khan M (2012) Mesenchymal stem cells for cardiac regeneration: translation to bedside reality. *Stem Cells Int.* **2012**, 1–14.
22 Allers C, Sierralta WD, Neubauer S, Rivera F, Minguell JJ, Conget PA (2004) Dynamic of distribution of human bone marrow-derived mesenchymal stem cells after transplantation into adult unconditioned mice. *Transplantation* **78**, 503–508.
23 Humes HD (2005) Stem cells: the next therapeutic frontier. *Trans. Am. Clin. Climatol. Assoc.* **116**, 167.
24 Niland S, Cremer A, Fluck J, Eble JA, Krieg T, Sollberg S (2001) Contraction-dependent apoptosis of normal dermal fibroblasts. *J. Invest. Dermatol.* **116**, 686–692.
25 Aizawa Y, Owen SC, Shoichet MS (2012) Polymers used to influence cell fate in 3D geometry: new trends. *Prog. Polym. Sci.* **37**, 645–658.
26 Hosseinkhani H, Hong PD, Yu DS (2013) Self-assembled proteins and peptides for regenerative medicine. *Chem. Rev.* **113**, 4837–4861.
27 Tashiro KI, Sephel GC, Weeks B, Sasaki M, Martin GR, Kleinman HK *et al.* (1989) A synthetic peptide containing the IKVAV sequence from the A chain of laminin mediates cell attachment, migration, and neurite outgrowth. *J. Biol. Chem.* **264**, 16174–16182.
28 Graf J, Iwamoto Y, Sasaki M, Martin GR, Kleinman HK, Robey FA *et al.* (1987) Identification of an amino acid sequence in laminin mediating cell attachment, chemotaxis, and receptor binding. *Cell* **48**, 989–996.
29 Adams DN, Kao EYC, Hypolite CL, Distefano MD, Hu WS, Letourneau PC (2005) Growth cones turn and migrate up an immobilized gradient of the laminin IKVAV peptide. *J. Neurobiol.* **62**, 134–147.
30 Takahashi Y, Tabata Y (2003) Homogeneous seeding of mesenchymal stem cells into nonwoven fabric for tissue engineering. *Tissue Eng.* **9**, 931–938.
31 Ma T, Li Y, Yang ST, Kniss DA (2000) Effects of pore size in 3-D fibrous matrix on human trophoblast tissue development. *Biotechnol. Bioeng.* **70**, 606–618.
32 Both SK, Muijsenberg AJVD, Blitterswijk CAV, Boer JD, Bruijn JDD (2007) A rapid and efficient method for expansion of human mesenchymal stem cells. *Tissue Eng.* **13**, 3–9.
33 Hosseinkhani H, Hosseinkhani M, Tian F, Kobayashi H, Tabata Y (2006) Osteogenic differentiation of mesenchymal stem cells in self-assembled peptide-amphiphile nanofibers. *Biomaterials* **27**, 4079–4086.
34 Hosseinkhani H, Hosseinkhani M, Tian F, Kobayashi H, Tabata Y (2006) Ectopic bone formation in collagen sponge self-assembled peptide–amphiphile nanofibers hybrid scaffold in a perfusion culture bioreactor. *Biomaterials* **27**, 5089–5098.
35 Rice JJ, Martino MM, De Laporte L, Tortelli F, Briquez PS, Hubbell JA (2013) Engineering the regenerative microenvironment with biomaterials. *Adv. Healthc. Mater.* **2**, 57–71.
36 Hosseinkhani H, Hosseinkhani M, Khademhosseini A, Kobayashi H (2007) Bone regeneration through controlled release of bone morphogenetic protein-2 from 3-D tissue engineered nano-scaffold. *J. Control. Release* **117**, 380–386.
37 Hosseinkhani H, Hosseinkhani M, Khademhosseini A, Kobayashi H, Tabata Y (2006) Enhanced angiogenesis through controlled release of basic fibroblast growth factor from peptide amphiphile for tissue regeneration. *Biomaterials* **27**, 5836–5844.
38 Santiago LY, Nowak RW, Peter Rubin J, Marra KG (2006) Peptide-surface modification of poly (caprolactone) with laminin-derived sequences for adipose-derived stem cell applications. *Biomaterials* **27**, 2962–2969.
39 Yu LM, Kazazian K, Shoichet MS (2007) Peptide surface modification of methacrylamide chitosan for neural tissue engineering applications. *J. Biomed. Mater. Res. A* **82**, 243–255.
40 Kasai S, Ohga Y, Mochizuki M, Nishi N, Kadoya Y, Nomizu M (2004) Multifunctional peptide fibrils for biomedical materials. *Pept. Sci.* **76**, 27–33.
41 Hosseinkhani H, Hiraoka Y, Li CH, Chen YR, Yu DS, Hong PD *et al.* (2013) Engineering 3D collagen-IKVAV matrix to mimic neural microenvironment. *ACS Chem. Neurosci.* **4**, 1229–1235.
42 Matsuda A, Kobayashi H, Itoh S, Kataoka K, Tanaka J (2005) Immobilization of laminin peptide in molecularly aligned chitosan by covalent bonding. *Biomaterials* **26**, 2273–2279.
43 Tysseling-Mattiace VM, Sahni V, Niece KL, Birch D, Czeisler C, Fehlings MG *et al.* (2008) Self-assembling nanofibers inhibit glial scar formation and promote axon elongation after spinal cord injury. *J. Neurosci.* **28**, 3814–3823.
44 Jongpaiboonkit L, King WJ, Murphy WL (2008) Screening for 3D environments that support human mesenchymal stem cell viability using hydrogel arrays. *Tissue Eng. Part A* **15**, 343–353.
45 Singh A, Elisseeff J (2010) Biomaterials for stem cell differentiation. *J. Mater. Chem.* **20**, 8832–8847.
46 Cooke MJ, Vulic K, Shoichet MS (2010) Design of biomaterials to enhance stem cell survival when transplanted into the damaged central nervous system. *Soft Matter* **6**, 4988–4998.
47 Kubinová Š, Horák D, Kozubenko N, Vaněček V, Proks V, Price J *et al.* (2010) The use of superporous Ac-CGGASIKVAVS-OH-modified PHEMA scaffolds to promote cell adhesion and the differentiation of human fetal neural precursors. *Biomaterials* **31**, 5966–5975.
48 Schaeffer HJ, Weber MJ (1999) Mitogen-activated protein kinases: specific messages from ubiquitous messengers. *Mol. Cell. Biol.* **19**, 2435–2444.

49 Schmitz KJ, Wohlschlaeger J, Lang H, Sotiropoulos GC, Malago M, Steveling K *et al.* (2008) Activation of the ERK and AKT signalling pathway predicts poor prognosis in hepatocellular carcinoma and ERK activation in cancer tissue is associated with hepatitis C virus infection. *J. Hepatol.* **48**, 83–90.

50 Franke TF (1999) A difficult Akt to follow. *Neural Notes* **5**, 3–7.

51 Franke TF, Kaplan DR, Cantley LC (1997) PI3K: downstream AKT ion blocks apoptosis. *Cell* **88**, 435.

52 Jones NC, Fedorov YV, Rosenthal RS, Olwin BB (2001) ERK1/2 is required for myoblast proliferation but is dispensable for muscle gene expression and cell fusion. *J. Cell. Physiol.* **186**, 104–115.

53 Coolican SA, Samuel DS, Ewton DZ, McWade FJ, Florini JR (1997) The mitogenic and myogenic actions of insulin-like growth factors utilize distinct signaling pathways. *J. Biol. Chem.* **272**, 6653–6662.

54 Choi SC, Kim SJ, Choi JH, Park CY, Shim WJ, Lim DS (2008) Fibroblast growth factor-2 and-4 promote the proliferation of bone marrow mesenchymal stem cells by the activation of the PI3K-Akt and ERK1/2 signaling pathways. *Stem Cells Dev.* **17**, 725–736.

55 Ryu CH, Park SA, Kim SM, Lim JY, Jeong CH, Jun J *et al.* (2010) Migration of human umbilical cord blood mesenchymal stem cells mediated by stromal cell-derived factor-1/CXCR4 axis via Akt, ERK, and p38 signal transduction pathways. *Biochem. Biophys. Res. Commun.* **398**, 105–110.

56 Li B (2012). Isolation of BMMSCs and its Effect on Spinal Cord Repair Materials [D]. Wuhan: Wuhan University of Technology. (in Chinese).

57 Yuan T (2012). Preparation and Characterization of YIGSR and IKVAV Peptides Grafted Hydrogel [D]. Wuhan: Wuhan University of Technology. (in Chinese).

58 Alessi DR, Cuenda A, Cohen P, Dudley DT, Saltiel AR (1995) PD98059 is a specific inhibitor of the activation of mitogen activated protein kinase in vitro and in vivo. *J. Biol. Chem.* **270**, 27489–27494.

59 Wipf P, Halter RJ (2005) Chemistry and biology of wortmannin. *Org. Biomol. Chem.* **3**, 2053–2061.

60 Ranieri JP, Bellamkonda R, Bekos EJ, Gardella JA Jr, Mathieu HJ, Ruiz L *et al.* (1994) Spatial control of neuronal cell attachment and differentiation on covalently patterned laminin oligopeptide substrates. *Int. J. Dev. Neurosci.* **12**, 725–735.

61 Smith MW, Newey JM (1960) Amino acid and peptide transport across the mammalian small intestine. *Protein Melab. Nutr.* **64**, 213–219.

62 Zhu J (2010) Bioactive modification of poly (ethylene glycol) hydrogels for tissue engineering. *Biomaterials* **31**, 4639–4656.

63 Drury JL, Mooney DJ (2003) Hydrogels for tissue engineering: scaffold design variables and applications. *Biomaterials* **24**, 4337–4351.

64 Shekaran A, Garcia AJ (2011) Nanoscale engineering of extracellular matrix-mimetic bioadhesive surfaces and implants for tissue engineering. *Biochim. Biophys. Acta*, **1810**, 350–360.

65 Elbert DL, Hubbell JA (1996) Surface treatments of polymers for biocompatibility. *Annu. Rev. Mater. Sci.* **26**, 365–294.

66 Zou Z, Zheng Q, Wu Y, Song Y, Wu B (2009) Growth of rat dorsal root ganglion neurons on a novel self-assembling scaffold containing IKVAV sequence. *Mater. Sci. Eng., C* **29**, 2099–2103.

67 Lévesque SG, Shoichet MS (2006) Synthesis of cell-adhesive dextran hydrogels and macroporous scaffolds. *Biomaterials* **27**, 5277–5285.

68 Cui FZ, Tian WM, Fan YW, Hou SP, Xu QY, Lee IS (2003) Cerebrum repair with PHPMA hydrogel immobilized with neurite-promoting peptides in traumatic brain injury of adult rat model. *J. Bioact. Compat. Polym.* **18**, 413–432.

69 Tysseling-Mattiace VM, Sahni V, Niece KL, Birch D, Czeisler C, Fehlings MG *et al.* (2008) Self-assembling nanofibers inhibit glial scar formation and promote axon elongation after spinal cord injury. *J. Neurosci.* **28**, 3814–3823.

70 Wu B, Zheng Q, Wu Y, Guo X, Zou Z (2010) Effect of IKVAV peptide nanofiber on proliferation, adhesion and differentiation into neurocytes of bone marrow stromal cells. *J. Huazhong Univ. Sci. Technol. Med. Sci.* **30**, 178–182.

71 Li X, Liu L, Meng D, Wang D, Zhang J, Shi D *et al.* (2012) Enhanced apoptosis and senescence of bone-marrow-derived mesenchymal stem cells in patients with systemic lupus erythematosus. *Stem Cells Dev.* **21**, 2387–2394.

72 Sasaki K, Kurose A, Ishida Y (1993) Flow cytometric analysis of the expression of PCNA during the cell cycle in HeLa cells and effects of the inhibition of DNA synthesis on it. *Cytometry* **14**, 876–882.

73 Hall PA, Levison DA, Woods AL, Yu CW, Kellock DB, Watkins JA *et al.* (1990) Proliferating cell nuclear antigen (PCNA) immunolocalization in paraffin sections: an index of cell proliferation with evidence of deregulated expression in some, neoplasms. *J. Pathol.* **162**, 285–294.

74 Steelman LS, Pohnert SC, Shelton JG, Franklin RA, Bertrand FE, McCubrey JA (2004) JAK/STAT, Raf/MEK/ERK, PI3K/Akt and BCR-ABL in cell cycle progression and leukemogenesis. *Leukemia* **18**, 189–218.

75 Peng CY, Pan SL, Huang YW, Guh JH, Chang YL, Teng CM (2008) Baicalein attenuates intimal hyperplasia after rat carotid balloon injury through arresting cell-cycle progression and inhibiting ERK, Akt, and NF-κB activity in vascular smooth-muscle cells. *Naunyn Schmiedeberg's Arch. Pharmacol.* **378**, 579–588.

76 Bernardi RJ, Trump DL, Yu WD, McGuire TF, Hershberger PA, Johnson CS (2001) Combination of 1α, 25-dihydroxyvitamin D3 with dexamethasone enhances cell cycle arrest and apoptosis role of nuclear receptor cross-talk and Erk/Akt signaling. *Clin. Cancer Res.* **7**, 4164–4173.

77 Roy SK, Srivastava RK, Shankar S (2010) Inhibition of PI3K/AKT and MAPK/ERK pathways causes activation of FOXO transcription factor, leading to cell cycle arrest and apoptosis in pancreatic cancer. *J. Mol. Signal.* **5**, 10.

78 Chang L, Karin M (2001) Mammalian MAP kinase signaling cascades. *Nature* **410**, 37–40.

79 Dhennin-Duthille I, Masson M, Damiens E, Fillebeen C, Spik G, Mazurier J (2000) Lactoferrin upregulates the expression of CD4 antigen through the stimulation of the mitogen-activated protein kinase in the human lymphoblastic T Jurkat cell line. *J. Cell. Biochem.* **79**, 583–593.

80 Yamamoto T, Ebisuya M, Ashida F, Okamoto K, Yonehara S, Nishida E (2006) Continuous ERK activation downregulates antiproliferative genes throughout G1 phase to allow cell-cycle progression. *Curr. Biol.* **16**, 1171–1182.

81 Shin I, Yakes FM, Rojo F, Shin NY, Bakin AV, Baselga J *et al.* (2002) PKB/Akt mediates cell-cycle progression by phosphorylation of p27Kip1 at threonine 157 and modulation of its cellular localization. *Nat. Med.* **8**, 1145–1152.

82 Brunet A, Bonni A, Zigmond MJ, Lin MZ, Juo P, Hu LS *et al.* (1999) Akt promotes cell survival by phosphorylating and inhibiting a Forkhead transcription factor. *Cell*, **96**, 857–868.

83 Bravo R (1986) Synthesis of the nuclear protein cyclin (PCNA) and its relationship with DNA replication. *Exp. Cell Res.* **163**, 287–293.

84 Celis JE, Celis A (1985) Individual nuclei in polykaryons can control cyclin distribution and DNA synthesis. *EMBO J.* **4**, 1187.